Design and Performance Comparison of Compact Resonant Cavity Antennas Using Customized 3D Printing Techniques

Touseef Hayat*, Muhammad U. Afzal†, Foez Ahmed†, Karu P. Esselle†,
School of Engineering, Macquarie University, Sydney, Australia, touseef.hayat@mq.edu.au
†School of Electrical and Data Engineering, University of Technology Sydney, Sydney, Australia

***Abstract*—The Far-field radiation performance of quintessential compact resonant cavity antennas (CRCAs) is compromised because of even transmission through uniform superstrate resulting in non-uniform aperture phase distribution. Phase varying superstrate (PVS) can be used to improve uniformity in aperture phase distribution and hence attain wideband directional performance of CRCAs with small footprint. This paper demonstrates customization ability of additive manufacturing (AM) by designing three PVSs for CRCA using distinct fabrication approaches. The printing methodologies are based on height variation, infill variation, and perforation size variation in the RF graded acrylo-butadiene styrene (ABS) material. Each PVS comprises three dielectric regions with non-identical electrical propoerties to locally vary input phase of antenna. Uneven transmission through PVSs remarkably improves the aperture phase error of CRCAs, and achieves high-directivity (>17 dB) and wide bandwidth (>50%) with a small footprint of ≈0.84λ_L in diameter at the lowest operating frequency.**

***Index Terms*—3D printing, acrylo-butadiene styrene (ABS), additive manufacturing, rapid prototyping, resonant cavity antenna (RCA), wideband compact antenna.**

I. Introduction

High-gain ultra-wideband antenna systems with simple and compact configurations are highly in demand for 5G communication systems. Compact resonant cavity antennas (CRCAs) have drawn unprecedented interest in recent years because despite planar configuration and simple feeding mechanism, they can achieve high-gain (16-20 dB) and large bandwidth (>50%) with small footprint [1], [2], [3]. CRCAs comprise a resonant cavity formed between a traditional low-gain feed antenna and partially reflecting superstrate (PRS) [4]. The cavity resonates at the operating frequency thus resulting in enhanced directional radiation. Researchers have investigated that CRCAs have inherently non-uniform aperture-phase distribution, which limits their optimal performance [4], [5]. Several techniques have been proposed to modify constituent elements of the cavity to improve performance figures of CRCAs. These techniques primarily include modifications to the superstrate [6].

The concept of wideband highgain CRCA with multilayered superstrate was proposed in 2014 [1]. The superstructure comprised three dielectric slabs, and thicknesses of slabs were tuned to attain wideband characteristics of the antenna. This antenna demonstrated the peak gain of 18.2 dB and 3 dB directivity bandwidth of 22% with a small aperture area of $2.25\lambda_L^2$. Later on, to achieve directivity bandwidth in excess of 50%, CRCAs with single-layered transverse permittivity gradient superstrate (TPGS) were presented [2]. Peak directivity of 16.4 dB and directivity bandwidth of 52.9% was achieved with footprint area of $1.54\lambda_L^2$ at the lowest operating frequency. In following years, few numerical techniques like paricle swarm optimization and cross-entropy were implemented to optimize TPGS to improve sidelobe levels and achieve peak directivity >20 dB while maintaining directivity bandwidth >50 dB [3], [7]. The previously discussed designs met the performance requirements but their wide-scale adoptation was unrealistic because permittivity distribution profile in TPGS was achieved using commercial laminates, which come with preset permittivity values. Hence numerical optimization techniques and prototyping was limited to a discrete set of permittivity values.

In the past decade, all superstrates reported for the wideband performance of CRCAs were machined from commercially available dielectric materials using traditional subtractive manufacturing (SM) techniques such as CNC machining [1], [2], [3], [7], [8]. This method is both expensive and sedate as milling and machining using several drill bits wastes a massive amount of material. Moreover, with SM, it is not possible to model various geometries including unorthodox holes, unrealistic overhangs, and square perforations [9]. Hence all prior cited superstrates have elevated costs (a few hundred dollars), large build time, and minimal room for customization, which limit their wide-scale application. These limitations can be addressed by exploiting low-cost, rapid prototyping, and high customization abilities of additive manufacturing (AM) technique. This paper presents the modeling of three different phase varying superstrates (PVSs) for CRCA using distinct 3D printing techniques. Instead of using several dielectric materials, single RF graded PREPERM®ABS450 material with permittivity 4.4 (ε_r=4.4) is used to synthesize superstrates. The first superstrate has stepped dielectric geometry achieved by adjusting the height of PREPERM®ABS450 material in three sections of the Standard Tessellation Language (.stl) file imported for the print process. In the second PVS, the effective permittivity gradient is achieved by using multiple print processes having different infill percentages of PREPERM®ABS450 filament in circular regions of the superstrate. Phase variation in the third superstrate is achieved

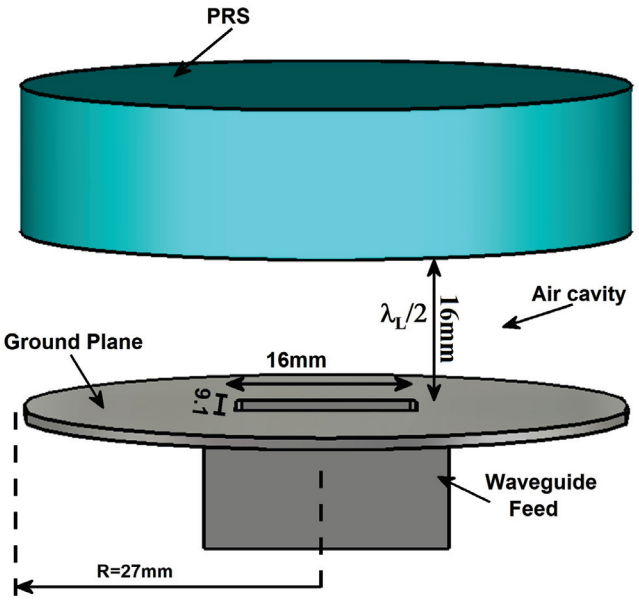

Fig. 1: Configuration of waveguide fed compact resonant cavity antenna with uniform superstrate.

by introducing square perforations of appropriate size in three sections. All three superstrates can be synthesized in less than 1 hour with an equivalent material cost of 1.25$. Wideband performance of CRCAs with proposed low-cost superstrates is comparable to any of their earlier reported expensive counterparts.

The rest of the paper has been organized into five sections including an introduction and a conclusion section. In Section II, we will explain the configuration of CRCA with a uniform superstrate. Section III explains the design and synthesis of three PVSs using fused deposition modeling (FDM) technique, while detailed discussion on results is presented in Section IV.

II. Antenna Configuration

Traditional CRCAs comprises an air-filled half wavelength ($\lambda_0/2$) spaced cavity formed between a perfect electric conductor ground plane and a uniform PRS. This cavity is excited by traditional low gain feed antenna such as patch or waveguide feed. The basic configuration of CRCA is shown in Fig. 1, in which a uniform superstrate is suspended at a spacing of 16 mm ($\approx\lambda_L/2$) over the ground plane, which is a condition for the ideal resonance of CRCA to attain optimal radiation performance [4], [5]. The ground is a metal sheet of radius R = 27 mm ($\approx 0.84\lambda_L$), which has a rectangular feeding slot (16 mm $\times$ 9.1 mm) in the middle, for the WR-75 waveguide adapter. Such CRCAs made from uniform superstrates are known to have non-uniform aperture phase distribution outside the cavity because of the patch delay experienced by the radiation response in different sections of antenna [2], [6]. Path delay can be compensated by tailoring transmission characteristics of PRS in different regions. This paper focuses on developing three extremely low-cost varying

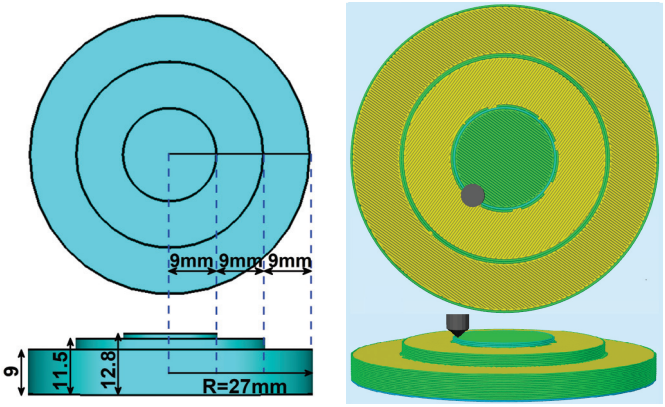

(a) (b)

Fig. 2: Top and side views of (a) simulated model and (b) preview mode of synthesised model of stepped superstrate.

phase delay superstrates to compensate phase error of CRCAs. The following section explains the design and synthesis of PVSs for CRCA.

III. Design and Synthesis of Superstrates

Phase variation in three superstrates will be achieved by height variation, infill variation, and perforation inclusion in PREPERM®ABS450 filament. Unlike traditional superstrates, all presented PVSs can be rapidly prototyped from single material using FDM technique. Each superstrate has three concentric rings of equal width of 9 mm and electrically different materials. Concentric rings were considered because of circular symmetry in aperture phase error of cavity antennas [4]. The number of concentric rings was set to three because excessively increasing the number of rings does not influence the performance significantly, rather it complicates the synthesis process [2]. In this design, we considered the circular aperture of size $\approx 0.84\lambda_L$ (27 mm), where λ_L is the free-space wavelength at the lowest operating frequency (9.2 GHz). The following subsections discuss the design and synthesis of PVSs.

A. Stepped Superstrate

Phase variation in this superstrate is achieved by staircase profile and the thickness reduces in three steps from center to edges. Contrary to traditional designs in which various commercially available dielectric slabs were combined using a standard ceramic cutting process, the height variation in the proposed superstrate is achieved by combining three concentric rings in the print process. The heights of three concentric rings were selected through parametric study, which for brevity is not presented here [10]. The optimal parameters values for height are h_1= 12.8 mm, h_2= 11.5 mm and h_3= 9 mm. The top and side view of the simulated model of stepped dielectric is shown in Fig. 2(a). Each simulated ring with different height was exported as a separate .stl file and one solid outline/perimeter shell was introduced at the outskirts of each ring to join all the .stls using simplify3D software.

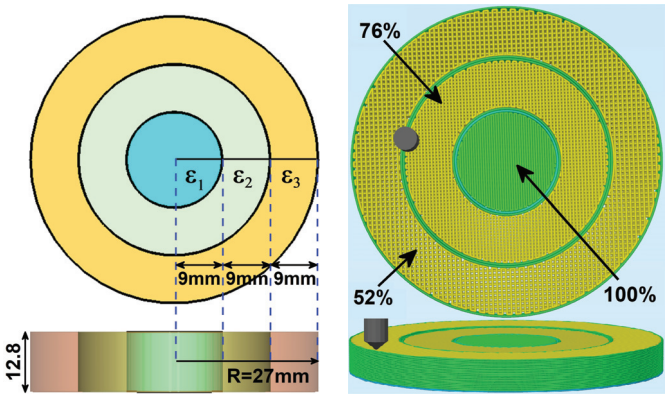

(a) (b)

Fig. 3: Top and side views of (a) simulated model and (b) preview mode of synthesised model of infill varying superstrate.

For synthesis, the layer height in the print process was set to 0.3 mm and an infill percentage of 100% was specified. The software statistics estimated build time of 58 minutes with material cost and weight of US$ 1.25 and 27.3 g respectively. A cross-sectional view screenshot captured during the print setup indicating the top and side view of the synthesized model is presented in Fig. 2(b).

B. Infill Superstrate

Phase variation in this superstrate is achieved by introducing a transverse permittivity gradient in the planar dielectric material. Contrary to traditional TPGSs made out of multiple commercial laminates, the proposed superstrate achieves an effective permittivity gradient using multiple print processes with different infill percentages, of the same dielectric filament. The effective permittivity of three concentric rings is selected through parametric study, as explained in [2], [6]. The optimal effective permittivity values for CRCA under consideration are ε_1= 4.4, ε_2= 3.6 and ε_3= 2.8. The top and side view of the simulated model of stepped dielectric is shown in Fig. 3(a). It has been reported that effective permittivity is linearly related to the infill fraction of 3D printed sample [6].

$$v_i = \frac{\varepsilon_{reff} - 1}{\varepsilon_r - 1} \tag{1}$$

where, v_i is the infill fraction, ε_{reff} is the effective permittivity of printed sample and ε_r is the permittivity of filament being used for printing, which is PREPERM®ABS450 here. Using eq. 1, the resultant infill percentages for effective permittivities 4.4, 3.6 and 2.8 were 100%, 76% and 52%. Three rings of the simulated file were exported as separate .stl files from CST studio Suite. The .stl files were imported in Simplify3D software and separate processes were added against each file with their corresponding infill percentages. A solid outline/perimeter shell was introduced at the edge of each ring to join all the .stls. For synthesis, the layer height in the print process was set to 0.3 mm, and software statistics estimated a build time of 58 minutes with material cost and weight of US$ 1.19 and 25.82 g. A cross-sectional view screenshot captured during the print setup indicating top and side view of synthesized model is presented in Fig. 3(b).

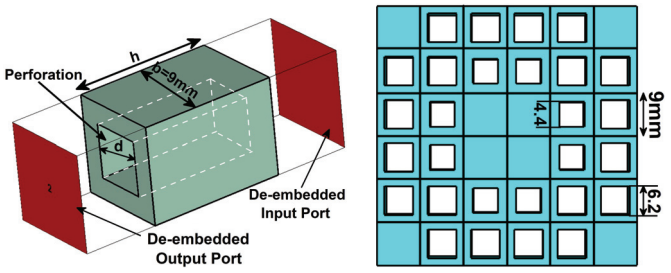

(a) (b)

Fig. 4: Top and side views of (a) simulated model and (b) preview mode of synthesised model of perforated superstrate.

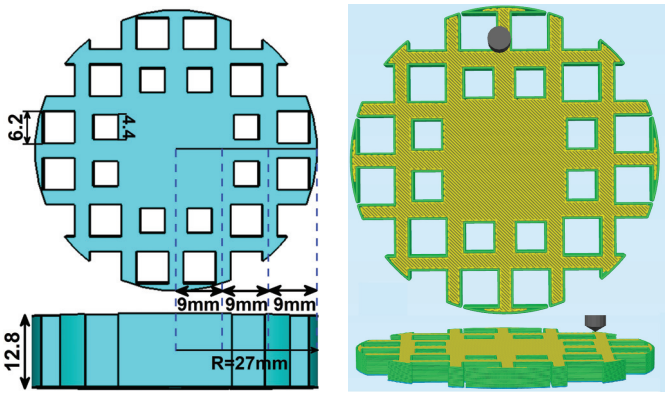

(a) (b)

Fig. 5: Top and side views of (a) simulated model and (b) preview mode of synthesised model of perforated superstrate.

C. Perforated Superstrate

It has been investigated that variation in perforation size tailors transmission phase through a dielectric block [9]. This concept has been utilized to design planar superstrate with square perforations in PREPERM®ABS450. Square perforations are particularly used because they offer a superior transmission phase compared to traditional circular drills [9]. A cuboid unit-cell with periodicity *b*, air perforation *d* and height *h* is shown in Fig. 4. The effective permittivity of such unit-cell can be calculated using the following expression:

$$\varepsilon_{reff} = \frac{D_k vol \times \varepsilon_d + Perf vol \times \varepsilon_a}{UC vol} \tag{2}$$

where, ε_{reff} is effective permittivity of sample, D_k vol is the volume of dielectric, Perf vol is the volume of air perforation and UC vol is the total volume of unit cell. Using mathematical formula for volume of cuboid, eq. 2 can be re-written as:

$$\varepsilon_{reff} = \frac{[(b^2 - d^2)] \times \varepsilon_d + (d^2) \times \varepsilon_a}{b^2} \tag{3}$$

since the effective permittivities of three concentric rings are known from the design of the second superstrate, those values

TABLE I: Build statistics comparison for all three PVSs.

Superstrate	Time (min)	Cost	Weight	Extruders	Length (m)	pp
Height	58	1.25	27.3	Single	9.1	1
Infill	58	1.19	25.8	Dual	8.9	3
Perforated	50	0.96	20.8	Single	6.9	1

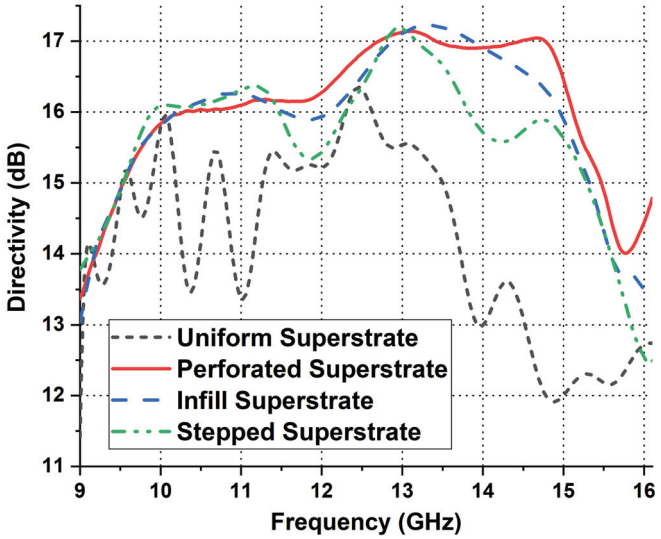

Fig. 6: Comparison of wideband directivity of CRCAs with PVSs and uniform superstrate.

can be utilized to design perforated unit-cells with transmission phases identical to the material with corresponding effective permittivity. The periodicity of the unit-cell will be equal to the width of the concentric ring of superstrate i.e. *9 mm* and height will be equivalent to that of the second superstrate (h=12.8 mm). To calculate perforation size (b) in unit-cell, eq. 3 can be modified as:

$$b^2 = \frac{(\varepsilon_{reff} \times a^2) - (a^2 \times \varepsilon_d)}{(1 - \varepsilon_d)} \tag{4}$$

using 4 we find that for ε_{reff}=4.4, ε_{reff}=3.6 and ε_{reff}=2.8 the corresponding perforation (b) values are p_1=0, p_2≈4.4 mm and p_3≈6.2 mm. Considering the circular symmetry in phase error of waveguide feed, the perforated unit cells were arranged in form of concentric circles to form a perforated superstrate. The arrangement of unit-cells is shown in Fig. 4(b). The arranged unit-cells were truncated to attain radial geometry equivalent to the size of antenna aperture (R=27mm). All unit-cells were joined to form a single superstrate. The top and side view of the simulated model of stepped dielectric is shown in Fig. 5(a). The simulated superstrate was exported as .stl file and 0.3 mm layer height was specified in the print setup to estimate build statistics in simplify3D. The software estimated build time of 50 minutes with material cost and weight of US$ 0.96 and 20.79 g. A cross-sectional view screenshot captured during the print setup indicating the top and side view of the synthesized model is presented in Fig. 5(b).

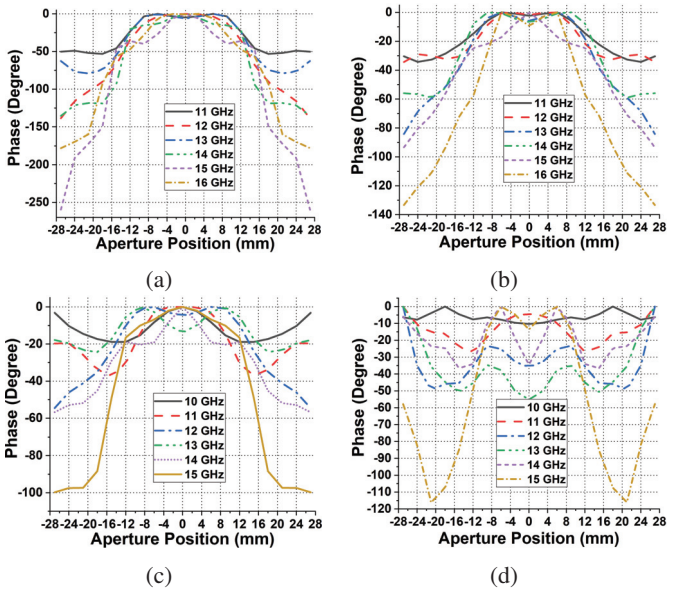

Fig. 7: E-Field distribution on aperture within operating band (a) uniform superstarte (b) height superstarte (c) infill superstarte (d) perforated superstarte.

In this way, all three superstrates were designed in CST Studio and synthesized using simplify3D, and their build statistics comparison based on build time, cost, weight, filament length, required print processes, and printer extruders are given in Table I. Proposed PVSs can be incorporated in CRCA to attain wideband directional performance. The next section provides a detailed performance analysis of three PVS-based CRCAs.

IV. Results and Discussion

Full-wave simulations of three CRCAs were performed in CST Microwave Studio. To highlight the superiority of CRCAs with PVSs, we also simulated CRCA with a uniform PREPERM®ABS450 superstrate. Comparison for wideband directivity for uniform superstrate and PVS-based RCAs is shown in Fig. 6. It can be noted that peak directivity with uniform superstrate is significantly lower than that with PVSs. Both CRCAs with infill variation and perforation size variation superstrates demonstrated the highest peak directivity of 17.23 dB. CRCA with stepped superstrate had peak directivity of 17 dB and with uniform superstrate had 16.4 dB. Respective half-power directivity bandwidths of CRCAs with infill variation, height variation, and perforation size variation are 51.6%, 51% and 50.8% compared to 22.6% demonstrated by CRCA with uniform superstrate. This is because of tremendous improvement in near-field aperture phase distribution of the CRCAs with the PVSs.

The electric field of all four CRCAs was probed 2 mm above the aperture planes and the phase variation of the dominant electrical field component of four simulated CRCAs taken at six different frequencies within the operating band is shown in Fig. 7 (a)-(d). From Fig 7, it is comprehended that within the operational band, CRCA with uniform superstrate has the

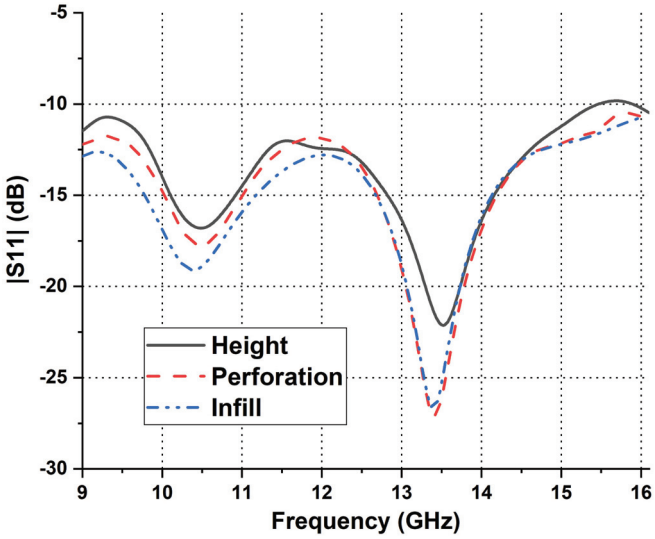

Fig. 8: Input reflection of CRCAs with PVSs

TABLE II: Performance comparison of PVS based CRCAS with recently published work.

Sup.	Peak Dir. (dB)	3dB Dir. BW (%)	SLL (dB)	Area (λ_L^2)	DBP	DBP/A
Height	17.20	51.0	10.9	1.8	2676.5	1487
Infill	17.23	50.8	14.3	1.8	2684.5	1491
Perf.	17.23	51.6	14.7	1.8	2726.8	1515
[2]	16.6	54.7	-10	1.54	2500.0	1623
[3]	20.7	56.0	-12	5.3	6662.0	1257
[7]	17.6	51.0	-10	2.69	2934.7	1091

highest phase error of 259.3°. The aperture phase error is lowest (≈100°) with an infill varying superstrate and hence it has peak half-power bandwidth. Respective phase errors for stepped superstrate and perforated superstate are 133.4° and 114.7°. The magnitude of input reflection coefficients of three CRCAs with PVSs is shown in Fig. 8. The magnitude of the reflection coefficient is less than -10 dB in the complete operational band for all three PVS-based CRCAs. To highlight the superiority of superstrates proposed in this paper, Table II compares the directive radiation performance of the proposed PVS-based CRCAs with some of the most recently published wideband CRCAs. The CRCA has matching performance with its counterparts in terms of directivity, sidelobe levels (SLLs), directivity bandwidth product (DBP), and DBP per unit Area (DBP/A). While it is developed at an only fractional cost to that required to prototype previously reported CRCAs.

V. Conclusion

The customization ability of AM has been demonstrated by rapid prototyping of three PVSs for CRCA. Superstrates have been synthesized by height variation, infill variation, and perforation size variation in PREPERM®ABS450 material. All three superstrates demonstrate demonstrate high-directivity (>17 dB) and wide bandwidth (>50%) with a small footprint area of $1.8\lambda_L^2$.

Acknowledgment

This research has been supported by and Australian Research Council Discovery garnt and the International Macquarie University Research Excellence Scholarship (iMQRES) No. 2017062/20181097.

References

[1] R. M. Hashmi, B. A. Zeb and K. P. Esselle, "Wideband High-Gain EBG Resonator Antennas With Small Footprints and All-Dielectric Superstructures," in IEEE Transactions on Antennas and Propagation, vol. 62, no. 6, pp. 2970-2977, June 2014, doi: 10.1109/TAP.2014.2314534.

[2] R. M. Hashmi and K. P. Esselle, "A Class of Extremely Wideband Resonant Cavity Antennas With Large Directivity-Bandwidth Products," in IEEE Transactions on Antennas and Propagation, vol. 64, no. 2, pp. 830-835, Feb. 2016, doi: 10.1109/TAP.2015.2511801.

[3] A. A. Baba, R. M. Hashmi and K. P. Esselle, "Achieving a Large Gain-Bandwidth Product From a Compact Antenna," in IEEE Transactions on Antennas and Propagation, vol. 65, no. 7, pp. 3437-3446, July 2017, doi: 10.1109/TAP.2017.2700016.

[4] M. U. Afzal, K. P. Esselle and B. A. Zeb, "Dielectric Phase-Correcting Structures for Electromagnetic Band Gap Resonator Antennas," in IEEE Transactions on Antennas and Propagation, vol. 63, no. 8, pp. 3390-3399, Aug. 2015, doi: 10.1109/TAP.2015.2438332.

[5] T. Hayat, M. U. Afzal, A. Lalbakhsh and K. P. Esselle, "3-D-Printed Phase-Rectifying Transparent Superstrate for Resonant-Cavity Antenna," in IEEE Antennas and Wireless Propagation Letters, vol. 18, no. 7, pp. 1400-1404, July 2019, doi: 10.1109/LAWP.2019.2917767.

[6] T. Hayat, M. U. Afzal, F. Ahmed, S. Zhang, K. P. Esselle and Y. Vardaxoglou, "Low-Cost Ultrawideband High-Gain Compact Resonant Cavity Antenna," in IEEE Antennas and Wireless Propagation Letters, vol. 19, no. 7, pp. 1271-1275, July 2020, doi: 10.1109/LAWP.2020.2997966.

[7] M. Kovaleva, D. Bulger, B. A. Zeb and K. P. Esselle, "Cross-Entropy Method for Electromagnetic Optimization With Constraints and Mixed Variables," in IEEE Transactions on Antennas and Propagation, vol. 65, no. 10, pp. 5532-5540, Oct. 2017, doi: 10.1109/TAP.2017.2740974.

[8] A. A. Baba, R. M. Hashmi, K. P. Esselle and A. R. Weily, "Compact High-Gain Antenna With Simple All-Dielectric Partially Reflecting Surface," in IEEE Transactions on Antennas and Propagation, vol. 66, no. 8, pp. 4343-4348, Aug. 2018, doi: 10.1109/TAP.2018.2842247.

[9] T. Hayat, M. U. Afzal, A. Lalbakhsh and K. P. Esselle, "Additively Manufactured Perforated Superstrate to Improve Directive Radiation Characteristics of Electromagnetic Source," in IEEE Access, vol. 7, pp. 153445-153452, 2019, doi: 10.1109/ACCESS.2019.2948735.

[10] A. A. Baba, R. M. Hashmi, K. P. Esselle, Z. Ahmad and J. Hesselbarth, "Millimeter-Wave Broadband Antennas With Low Profile Dielectric Covers," in IEEE Access, vol. 7, pp. 186228-186235, 2019, doi: 10.1109/ACCESS.2019.2953861.